Proceedings of the Combustion Institute 41 (2025) 105835

Contents lists available at ScienceDirect

Proceedings of the Combustion Institute

journal homepage: www.elsevier.com/locate/proci

Experimental investigation and optimization of ammonia–hydrogen chemical kinetics with ignition delay times from shock tubes

Torsten Methling [a,*], Michael Pierro [b], Nikolas Hulliger [b], Justin J. Urso [b], Jakob Krämer [a], Clemens Naumann [a], Markus Köhler [a], Subith S. Vasu [b]

[a] German Aerospace Center (DLR), Institute of Combustion Technology, Stuttgart, Germany

[b] University of Central Florida, Center for Advanced Turbomachinery and Energy Research (CATER), Orlando, Florida, United States

ARTICLE INFO

Keywords:
Ammonia
Hydrogen
Ignition delay times
Shock tubes
Chemical kinetic modeling

ABSTRACT

A combined experimental and numerical approach investigates the ignition delay times of ammonia–hydrogen mixtures in oxygen or synthetic air measured in shock tubes under different dilutions with argon and nitrogen. A series of novel ignition delay time measurements is presented for stoichiometric fuel–air mixtures diluted 1:10 and 1:5 in argon as well as 1:2 in nitrogen at the shock tube facility of the German Aerospace Center (DLR). The initialized gas conditions behind the reflected shock waves range between 940–2200 K and 4–16 bar. Additionally, recent ignition delay time determinations of fuel–air mixtures without subsequent dilution from the shock tube facility of the University of Central Florida (UCF) are reevaluated. Experimental data sets are analyzed with the application of multiple chemical kinetic models. The study reveals deficiencies in the modeling of fuel-oxidizer mixtures with relatively low dilution, representative for real combustion applications. To improve the chemical kinetic modeling capabilities, the reaction model DLR Concise is updated with new insights from literature. Subsequently, the updated model is optimized with the new experimental data and additional data on ignition delay times available from literature. 373 ignition delay times of ammonia and its mixture with hydrogen are targeted for the optimization. The linear transformation model is applied to optimize the most sensitive N-chemistry reactions within their uncertainties. The new experimental data from DLR confirm the observed deviations between the reevaluated experimental data from UCF and established chemical kinetic models. The updated and optimized DLR Concise models are resolve these modeling deficiencies and consistently reproduce the new and reevaluated data from both shock tube facilities. The optimized reaction model consistently reproduces the complete targeted experimental data with a broad range of initial temperature, pressure and mixture boundary conditions. Thus, the model can reliably be applied for numerical investigations of internal combustion engine ignition processes.

1. Introduction

Ammonia is a major shipping commodity in the global transport sector. With this in mind, ammonia has gained attention as a potential non-carbon fuel for ammonia freighters – using their cargo as fuel – to further reduce the CO_2 footprint in the maritime sector. To facilitate the design of modern ammonia ship engines, i.e. internal combustion engines or gas turbines in hybrid electric propulsion systems, the combustion characteristics need to be studied in detail. For maritime internal combustion engines an essential combustion characteristic is the ignition delay time as a marker of the ignitability. Due to the low reactivity of ammonia, the ignition in internal combustion engines typically needs to be promoted, e.g. by carbon-based fuel pilot injection or hydrogen admixture. Therefore, a systematic understanding of ammonia and ammonia–hydrogen ignition process and its design in applied combustion requires detailed chemical kinetic insight.

Several experimental investigations on the ignition behavior of ammonia and its mixture with hydrogen have been conducted using shock tubes. To reduce experimental uncertainties, this type of experiment is often conducted under diluted conditions of fuel-oxidizer mixtures, e.g. to reduce the temperature increase due to heat release and reduce the impact of inhomogeneities [1,2]. The dilution thereby represents a tradeoff between data quality for chemical kinetic model development and data comparability to real combustion application conditions. Since temperature and partially pressure dependent reaction rate coefficients show similar sensitivities on ignition delay times (IDT), this tradeoff

* Corresponding author.
E-mail address: torsten.methling@dlr.de (T. Methling).

https://doi.org/10.1016/j.proci.2025.105835
Received 1 May 2025; Accepted 3 September 2025
Available online 24 September 2025

is often shifted towards data quality. Mathieu and Petersen [3] investigated ammonia ignition delay times for fuel equivalence ratios φ = 0.5–2.0 under highly diluted conditions with the mole fractions of argon X_{Ar} of 98% and 0.99%. The initialized temperatures ranged from 1500 K to 2500 K and pressures ranged from 4 bar to 25 bar. Chen et al. [4] investigated stoichiometric mixtures of ammonia and hydrogen, with hydrogen fuel mole fractions $X_{H2,fuel}$ of up to 70%. The fuel and oxygen mixture was diluted in argon with X_{Ar} = 92%. With the admixture of hydrogen and the lower dilution, Chen et al. [4] reached ignition for initialized temperatures as low as 1000 K and pressures between 1 bar and 13 bar. Baker et al. [5] investigated IDTs of fuel mixtures of hydrogen, ammonia and natural gas at stoichiometric conditions at the UCF shock tube facility. The investigated mixtures include one fuel mixture that only consists of ammonia and hydrogen with a 50/50 ratio. As a diluent, they used a mixture of argon and nitrogen to investigate the impact of nitrogen as a bath gas. In their work the total diluent mole fraction was approximately 97%. For the ammonia–hydrogen test mixture, IDTs were detected for initialized temperatures between approximately 1400 K and 1750 K at a pressure of 2 bar. To investigate ignition delay times under more realistic engine-like conditions, Pierro et al. [6] measured ignition delay times of ammonia and its mixtures with up to 50% hydrogen undiluted in air with φ = 0.5–1.5 at the shock tube facility of the University of Central Florida (UCF). This effectively relates to a dilution of the fuel–oxygen mixtures with X_{N2} between 53% and 69%. As a surprising result, no current chemical kinetic model is able to consistently reproduce these experimental results.

Various chemical kinetic combustion models for ammonia have been developed. Szanthoffer et al. [7] and Girhe et al. [8] evaluated numerous models on comprehensive, versatile experimental data sets, including ignition delay times, laminar burning velocities and speciation data from jet-stirred reactors, flow reactors and shock tubes. These evaluations point out that several chemical kinetic models can consistently model major fractions of the investigated experimental data sets. Ammonia models with good experimental agreements include the CRECK model [9], the KAUST model [10], the NUIG model [11]. Nevertheless, as stated before, these models are also not capable in consistently reproducing the experimental ignition delay times by Pierro et al. [6].

The objective of this work is the improvement of the chemical kinetic modeling of the ignition process of ammonia and its mixture with hydrogen. New experimental ignition delay time investigations were conducted in a shock tube for high-pressures of up to 16 bar and high-temperatures up to 2500 K, to broaden the boundary conditions of available IDT data. Mixtures of ammonia and hydrogen were investigated under diluted conditions in argon or nitrogen. For the nitrogen dilution case of the fuel–air mixtures, X_{Ar} was 80% and 90%. For the nitrogen dilution case, the fuel–air mixture was diluted 1:2 in nitrogen, which effectively corresponds to a fuel–oxygen mixture with X_{N2} = 80%. Thus, the new experimental data are in-between the dilution conditions of data available in literature and data from Pierro et al. [6]. A focus of this work is set on the modeling of the experimental data of Pierro et al. [6]. In a first step, the experimental boundary conditions were reevaluated — namely, the pressure rise before the ignition event. In a second step, our in-house model DLR Concise [12] was updated based on new findings on ammonia modeling from literature, significantly improving the reproducibility of the experimental data from Pierro et al. [6]. Finally, we conducted an optimization of the updated chemical kinetic model on the IDT data from this work as well as on IDT literature data, by applying the optimization framework of the linear transformation model (linTM) [13].

2. Experimental data

Different experimental ignition delay time data sets are studied in this work. The data sets consist of new IDT measurements from the DLR shock tube facility, reevaluated IDT data including pressure increases before ignition from the data of Pierro et al. [6], and a collections of IDTs measured with shock tubes from literature. The overall experimental data set is summarized in Table 1.

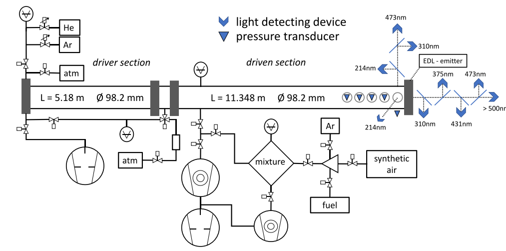

Fig. 1. Setup scheme of the DLR shock tube.

2.1. DLR shock tube

The shock tube as sketched in Fig. 1 has been detailed in previous publications also investigating ammonia decomposition [14,15]. Its driven section is well tempered to 353 K as well as the mixing vessel to 373 K. This reduces adsorption of water to the walls and thus prevents ammonia losses. The diagnostic section located close to the end wall (see Fig. 1) has four equally spaced and coated piezoelectric pressure transducers (PCB 112B05/RV-106) to record the time of arrival of the incident and reflected shock waves. The temperature and pressure immediately behind the incident and reflected shock waves are determined by solving the one-dimensional Rankine–Hugoniot shock equations. The uncertainty in temperature providing the incident shock velocity was analyzed to be within ±1.5% at 1000 K [15]. In addition, the relative uncertainty of the measured shock wave velocity for this shock tube is less than 1%. This translates to an uncertainty in T_5 ranging from ±15 K to ±40 K over the entire temperature range and an uncertainty in p_5 less than ±3%. The observation period for this shock tube is extended up to 12 ms by matching the impedances of the driver gas to the driven gas at the contact surface resulting in a post-shock compression (see non-reactive pressure profile in Fig. 2).

Ignition was monitored at the measurement plane located 10 mm from the end wall in two ways: (i) by measuring the pressure profile behind the reflected shock wave with a piezoelectric pressure transducer (Kistler 603B, shielded against thermal drift) and (ii) by measuring the emission signal radially (side-on, 2 mm slits directly behind the shock tube's exit, the other in front of the photomultiplier's entrance window) and axially (head-on, open view) of the excited OH* radicals observed at a wavelength of 310 nm (Newport 10BPF10-310, PMT Hamamatsu R3896, logarithmic amplifier FEMTO HLVA-100). IDT values were derived by measuring the time difference between the instance of formation of a reflected shock wave at the end wall (t = 0 s) and the time of occurrence of the maximum emission signal of excited OH* radicals at the radial port (side-on), shown in Fig. 2. The measured times were adjusted by a blast wave correction, incorporating the delay between the ignition at the end wall and the side-on detection. The relative error of the ignition delay time measurements is less than 1% at high temperatures to 3% at lowest temperatures due to long lasting and weaker emission intensities. For very short ignition delay times below 30 μs the uncertainty increases significantly to up to 30% due to uncertainties of the blast-wave correction.

Ammonia and the ammonia–hydrogen blends were mixed stoichiometrically with synthetic air (SynAir). For the 4 bar cases the fuels were neat ammonia and a 50/50 ammonia–hydrogen blend and the fuel–air mixture was diluted 1:10 and 1:5 in argon. For the 16 bar cases the fuels were neat ammonia and 92/8, 80/20 and 50/50 ammonia–hydrogen blends and the fuel–air mixture was diluted 1:2 in nitrogen. For modeling purposes of the 16 bar cases, the non-reactive pressure traces are given in the Supplementary Materials on the experimental data.

Table 1
Boundary conditions of the investigated shock tube ignition delay times.

$X_{H2,fuel}$	Oxidizer	φ	Dilution	Diluent	T_5/K	p_5/bar	Source
0–50	SynAir	1.0	1:10–1:2	Ar; N_2	942–2196	3.8–17.8	pw
0–50	SynAir	0.5–1.5	–	–	1018–1687	4.3–25.0	[6], reevaluated
0	O_2	0.5–2.0	1:100–1:50	Ar	1564–2489	1.3–30.8	[3]
0–70	O_2	1.0	1:12.5	Ar	1023–1957	1.0–12.8	[4]
50	O_2	1.0	1:30.8	Ar + N_2	1438–1725	2.0	[5]

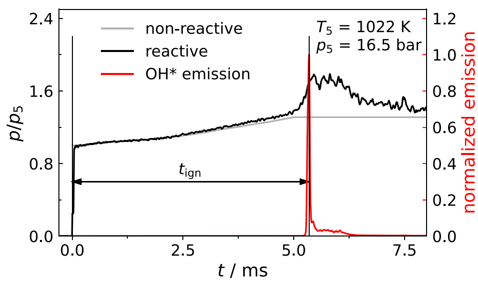

Fig. 2. Reactive and non-reactive pressure trace from DLR shock tube for the 50/50 ammonia–hydrogen mix at 16 bar.

2.2. UCF shock tube

The data collected from UCF [6] utilized the high-pressure shock tube at the HiPER-STAR facility [16]. The stainless-steel shock tube was designed to withstand pre-combustion pressures up to 1000 bar and has reached Mach numbers up to 15. The driven section is 8.54 m in length and has an internal diameter of 7.62 cm, allowing for high-pressure ignition studies while minimizing the effects of the boundary layer. Aluminum diagrams with thicknesses of 1.6 mm and scoring depths of 0.81 mm were ruptured to generate the shocks. Different ratios of He and N_2 were used to achieve the desired experimental conditions. Incident shock velocities were obtained by calculating the time between the pressure rise of five piezoelectric pressure transducers (PCB 113B23), which are equally spaced and span a distance of 1.9 m from the end wall. Before each experiment, an ultra-low vacuum (10^{-6} mbar) was achieved using a turbomolecular pump (Agilent TwisTorr 305S) to ensure mixture purity. All gases were supplied from Nexair (>99.999% purity) except NH_3, which was supplied by Linde (>99.995% purity). The mixtures were made in a Teflon-coated, stainless steel mixing tank and stirred using magnetic paddles for at least 1 h. Optical access is available 1 cm away from the end wall through side wall sapphire windows along with a side wall pressure transducer (PCB 113B23). A silicon optical receiver (Newport 2032) with a 306 nm (FWHM = 10 nm) narrow bandpass filter for OH* emission was used to determine IDTs, defined by the point of max slope traced down to baseline. Time zero was determined by extrapolating the reflected shock wave velocity back to the end wall.

For the data from prior work [6], the pressure increases $\mathrm{d}p/\mathrm{d}t$ were reevaluated before the ignition caused by gas dynamic effects. The values for the different experimental sets for $\mathrm{d}p/\mathrm{d}t$ were determined with a linear regression approach and are given in the Supplementary Materials SM2.

3. Modeling approach

The base chemical kinetic mechanism for this study is the DLR Concise [12,17]. This model is a semi-detailed mechanism with a design focus on real fuel modeling. The N-chemistry sub-model in this mechanism was taken from Glarborg et al. [18]. The DLR Concise is validated for a broad range of hydrogen, syngas and hydrocarbon fuels. Therefore, in this work, we did not change the O/H/C core mechanism and only updated the N-chemistry sub-model.

Major deviations between modeling results and experimental data from Pierro et al. [6] occur in an intermediate temperature regime below approximately 1200 K. Therefore, for the model update, a major focus is set on the HO_2 reaction chemistry, which has a major impact on the ignition process in the intermediate temperature regime [19, 20]. Jasper [21] investigated the third-body collision efficiencies and their temperature dependence of various collision partners in fall-off reactions. Among other findings, the author concluded that collision efficiency of NH_3 η_{NH3} can often be in the range of the collision efficiency of H_2O η_{H2O}, for which collision efficiency ratios to argon η_{H2O}/η_{Ar} are around the range of 10–20. Singal et al. [22] implemented into the chemical kinetic model of Alzueta et al. [23] the findings of Jasper [21] including a new temperature dependent mixing rule of rate coefficients LMR-R. With this implementation, Singal et al. [22] demonstrated a major impact of η_{NH3} on various targets of fundamental chemical kinetic investigations of mixtures of NH_3 and H_2. In our work, we identified a major impact on distinctive IDTs of η_{NH3} in reactions R1 and R2:

$$H + O_2(+M) \rightleftharpoons HO_2(+M) \tag{R1}$$

$$H_2O_2(+M) \rightleftharpoons OH + OH(+M) \tag{R2}$$

The reaction rates of R1 and R2 are typically sensitive in intermediate temperature ranges, which is also shown by the sensitivity analyses presented in the Supplementary Material SM2. R1 is forming HO_2, for which subsequent reaction steps lead to chain terminations, reducing reactivity. R1 is typically competing with the chain branching reaction $H + O_2 \rightleftharpoons OH + O$, contrarily increasing the reactivity. R2 is promoting reactivity by the decomposition of H_2O_2 into two OH radicals. The implementation of η_{NH3} in R1 and R2 has a major impact on the modeling results on data from Pierro et al. [6], shown in particular for R1 in Fig. 3. Based on the experimental agreement (Fig. 3), for η_{NH3}/η_{Ar} in R1 and R2 we assigned the values 10 and 8, respectively. For a more accurate estimation of these collision efficiencies, we included both as active parameters in the optimization process. Due to the limited temperature range of the targeted data in the optimization, the collision efficiencies were implemented as temperature independent constants, similar to the model by Jian et al. [24]. The optimization of temperature dependent third-body collision efficiencies, e.g. given for the LMR-R approach, should be included in large scale optimization in the future. Furthermore, since LMR-R is not yet part of the de facto standard Chemkin format, we decided to keep the constant values, to make the mechanism broadly applicable for the community, especially for CFD simulations.

The reactivity of ammonia is strongly influenced by the NH_2 reaction system [25]. In this context, Klippenstein and Glarborg [25] recently investigated the reaction $NH_2 + HO_2 \rightleftharpoons$ products using quantum mechanic approaches, being R3a–R3c and the subsequent reaction R4:

$$NH_2 + HO_2 \rightleftharpoons NH_3 + O_2 \tag{R3a}$$

$$\rightleftharpoons HNO + H_2O \tag{R3b}$$

$$\rightleftharpoons H_2NO + OH \tag{R3c}$$

$$H_2NO + OH \rightleftharpoons HNO + H_2O \tag{R4}$$

Accordingly, the DLR Concise was updated with their determined rate coefficients for R3 and R4. To further improve the overall modeling

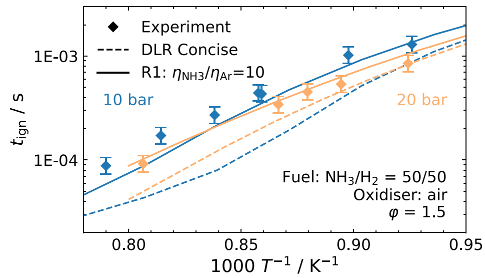

Fig. 3. The effect of η_{NH3} in R1 on ignition delay times measured by Pierro et al. [6].

performance on the experimental data set, the HO_2 reaction with ammonia R5 was updated with data from Stagni et al. [26]:

$$NH_3 + HO_2 \rightleftharpoons NH_2 + H_2O_2 \tag{R5}$$

Another NH_2 reaction pathway influencing the radical pool during the ignition process, is the NH_2 combination reaction forming diazene N_2H_2 and the subsequent chain branching reaction of N_2H_2 forming NNH and H:

$$NH_2 + NH_2 \rightleftharpoons N_2H_2 + H_2 \tag{R6}$$

$$N_2H_2(+M) \rightleftharpoons NNH + H(+M) \tag{R7}$$

Marshall et al. [27] conducted a theoretical investigation on the N_2H_2 system, including a new determination on the fall-off type reaction rate of R7. It should be noted that in the initial DLR Concise, only the low-pressure limit of R7 was implemented. For the updated model, the high-pressure limit and fall-off behavior was implemented from Marshall et al. [27], which significantly improved the model performance on the experimental data with a broad range of pressure conditions with different bath gases.

Updating the NH_2 sub-model not only affects ignition delay times, but also other combustion characteristics like laminar burning velocities or speciation data from fuel oxidations in different experimental devices. Even though, the focus of this work is the investigation of ignition delay times, we wanted to make sure that we do not over-optimize the developed mechanism towards a single kind of experimental data. The analysis of the N-chemistry sub-model in the DLR Concise from Glarborg et al. [18], revealed that ammonia laminar burning velocities are overestimated compared to experimental for many boundary conditions. We identified R8 and R9 having a major impact on the modeling results of laminar burning velocities:

$$NH_2 + NH \rightleftharpoons N_2H_2 + H \tag{R8}$$

$$HNO \rightleftharpoons H + NO \tag{R9}$$

By updating R8 and R9 to data from Klippenstein [28] and Stagni et al. [26], respectively, we were able to significantly improve the modeling performance in comparison to the experimental laminar burning velocities. The impacts of the sequential updates of R8 and R9 on the laminar burning velocities are shown in the Supplementary Material SM2.

To evaluate our newly developed model, we compare the modeling performance using different models from literature. Due to the comprehensive evaluation by Szanthoffer et al. [7] and Girhe et al. [8] we selected the models NUIG2023 [11], CRECK2023 [9] and KAUST2021 [10]. Due to the origin of the N-chemistry sub-model in the DLR Concise we compare the model to Glarborg2018 [18] and its updated version Glarborg2023 [29]. None of the above listed models in this paragraph incorporated the NH_3 collision efficiencies in reactions R1 and R2. Therefore, we also included the models Jian2024 [24] and Singal2024 [22], which consider NH_3 collision efficiencies.

4. Model optimization

For the optimization of the chemical kinetic model on the experimental data, we apply our in-house framework of the linear transformation model (linTM) [13,30]. A brief overview on the relevant steps of the linTM for this work is given below. For a detailed description of the linTM approach we refer to our prior work [13]. In this work the linTM optimization targets are the ignition delay times t_{ign}. The deviations between t_{ign} from experiments and modeling is given by the distance d defined as:

$$d = \Delta \ln t_{ign} = \ln(t_{ign,simulation}/t_{ign,target}) \tag{1}$$

In this study, only η_{NH3} and the pre-exponential factors A of the Arrhenius formulation for the rate coefficients are optimized. The pre-exponential factors were optimized within $\Delta \lg A = \pm 0.5$. This setting is based upon the comparison of different literature values of the rates and their uncertainties and suggestions from literature [31]. The optimization parameters are normalized with their corresponding maximum values to for the dimensionless optimization parameter τ. The linTM approach allows for a sufficient linearization of the relation between the targets and optimization parameters with the gradients $\partial d/\partial \tau$. The optimization problem is solved with a gradient based solver and the method of least squares. To analyze the model and identify the most important reactions of the overall optimization problem, the global sensitivity coefficient S_r for a reaction r defined by the linTM [13] is used.

For the parameter optimization the targets were the complete experimental set of 373 data points, given in Table 1. Depending on the given information for each experiment, the ignition delay times were simulated with given pressure profiles, pressure gradients dp/dt or constant pressure conditions. The simulations were conducted with the open-source software Cantera [32].

5. Results and discussion

A global sensitivity analysis with the linTM was conducted. The active optimization parameters were the pre-exponential factors of the eleven most sensitive reactions and the collision efficiencies η_{NH3} of R1, R2 and R17, totaling 16 optimization parameters. Table 2 summarizes the optimized reactions and their Arrhenius parameters with the exponential factor b, the activation energy E_A as well as the initial and optimized pre-exponential factor A_{init} and A_{opt}, respectively. The optimized collision efficiencies η_{NH3} of R1, R2 and R17 are 17.5, 15.9 and 3.6, respectively. To rule out an over-optimization of the reaction parameters, the optimized model is also validated against experimental data that are not the focus of this study. Brief comparisons of the updated and optimized model with experimental data for laminar burning velocities and speciation data from reactors are presented in the Supplementary Materials SM1.

Table 3 summarizes the performance of the different mechanisms with the indicator of their mean absolute distance $\bar{d}$ between the experimental and modeling results. This comparison shows that none of the models from literature, including the original DLR Concise, are unable to accurately, consistently reproduce the UCF data from Pierro et al. [6]. Among the literature models Glarborg2023 shows the best agreement for the UCF data. The sole integration of the collision efficiency of η_{NH3} in the models Jian2024 and Singal2024 does not lead to an consistent reproducibility of the UCF data. Among the literature models the NUIG2024 has the best performance on the DLR data and the complete data set *all*. With the update of the model DLR Concise with data from literature, the mean absolute distance $\bar{d}$ for all data is significantly reduced. Concretely, DLR Concise upd reproduces the UCF and the complete data set consistently, proving the validity of the UCF data. With the optimization, $\bar{d}$ of DLR Concise opt is further reduced for the complete data set. For a practical assessment of the

Table 2
Optimized reactions and their corresponding rate coefficients including the reference for the initial values, with E_A given in cal/mol and A given in combinations of cm, mol, s.

No.	Reaction		b	E_A	A_{init}	A_{opt}	Ref.
R3a	$NH_2 + HO_2 \rightleftharpoons NH_3 + O_2$		−1.910	−1 373.0	6.040e+18	1.506e+19	[25]
R5	$NH_3 + HO_2 \rightleftharpoons NH_2 + H_2O_2$		3.839	17 260.0	1.173e+00	1.847e+00	[26]
R7	$N_2H_2(+M) \rightleftharpoons NNH + H(+M)$	k_∞	0.000	63 980.0	6.300e+16	1.122e+16	[27]
		k_0	−6.910	70 400.0	8.700e+39	1.579e+39	
R10	$NH_3 + H \rightleftharpoons NH_2 + H_2$		2.230	10 400.0	2.538e+06	2.581e+06	[33]
R11	$NH_3 + OH \rightleftharpoons NH_2 + H_2O$		2.040	566.0	2.000e+06	8.321e+05	[34]
R12	$NH_2 + H(+M) \rightleftharpoons NH_3(+M)$	k_∞	0.000	0.0	1.600e+14	2.387e+14	[35]
		k_0	−1.760	0.0	3.600e+22	3.695e+22	
R13	$NH_2 + O_2 \rightleftharpoons H_2NO + O$		0.487	29 050.0	2.600e+11	2.121e+11	[36]
R14	$NH_2 + NO \rightleftharpoons NNH + OH$		0.294	−866.0	4.300e+10	3.478e+10	[37]
R15	$NH_2 + NO \rightleftharpoons N_2 + H_2O$		−2.369	870.0	2.600e+19	2.376e+19	[37]
R16	$NH_2 + NH_2 \rightleftharpoons NH_3 + NH$		3.530	552.0	5.600e+00	1.546e+01	[28]
R17	$NH + O_2 \rightleftharpoons HNO + O$		0.000	13 850.0	2.400e+13	5.143e+13	[18]

Table 3
Mean absolute distance $\bar{d}$ between targeted experiments and chemical kinetic results of investigated models.

Model	$\bar{d}$		
	UCF	*DLR*	*all*
Glarborg2018 [18]	0.569	0.434	0.390
Glarborg2023 [29]	0.305	0.289	0.313
Jian2024 [24]	0.671	0.280	0.390
Singal2024 [22]	0.475	0.283	0.341
CRECK2023 [9]	0.505	0.214	0.301
KAUST2021 [10]	0.403	0.325	0.389
NUIG2024 [11]	0.486	0.158	0.254
DLR Concise [17]	0.633	0.453	0.415
DLR Concise upd	0.162	0.183	0.183
DLR Concise opt	0.136	0.144	0.147

modeling quality, the complete performance of the models DLR Concise, DLR Concise upd and DLR Concise opt as well as the literature models Glarborg2023 and NUIG2024 is presented in the Supplementary Materials SM1. The results of the new experimental data and exemplary results for the data of Pierro et al. [6] are presented below.

Fig. 4 shows the experimental results and the effect on the modeling progression for the 4 bar cases diluted in Ar. For the 50/50 ammonia–hydrogen case, the effect of the model adaptations have a minor impact on the simulation results showing a slight increase of the predicted ignition delay times below 1200 K. This can be attributed to updated HO_2 reactions, becoming more relevant for intermediate temperatures, especially, reducing reactivity when introducing η_{NH3} to R1. Compared to the argon case, this effect becomes more accentuated for the ignition delay time measurements with N_2 as a bath gas under increased pressure, as observed ignition delay times are shifted towards lower temperatures, shown in Fig. 5. Under these dilution and pressure conditions, the original DLR Concise significantly under-predicts ignition delay times of the gas mixtures below approximately 1500 K. With the model adaptations, both the updated and optimized model are in excellent agreement with the experimental data, due to the reduced reactivity caused by R1.

The impact of the model adaptations on the simulation results of the data from Pierro et al. [6] is significant, demonstrated in Figs. 6 and 7. Both, the updated and optimized model agree with the experimental results and the findings are in line with the new experimental data discussed before. With the admixture of hydrogen to ammonia ignition delay times become faster and the observation range for the shock tube is shifted towards lower temperatures. Here, the intermediate temperature range and the low dilution are again impacted by the model adaptations for the HO_2, with a major contribution being the addition of η_{NH3} to R1. For ignition delay times of the rich 50/50 ammonia–hydrogen mixture, the modeling performances of all investigated mechanisms are demonstrated in Fig. 7. The only

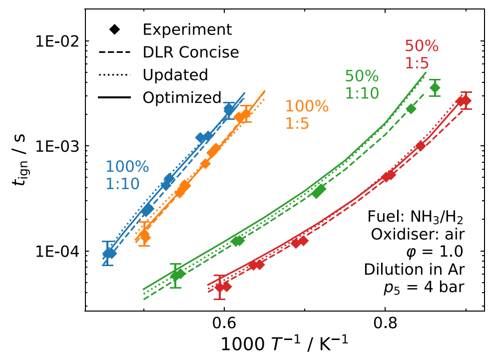

Fig. 4. Ignition delay times from DLR shock tube at 4 bar compared to modeling results with annotations referring to fuel hydrogen content $X_{H2,fuel}$ and dilution.

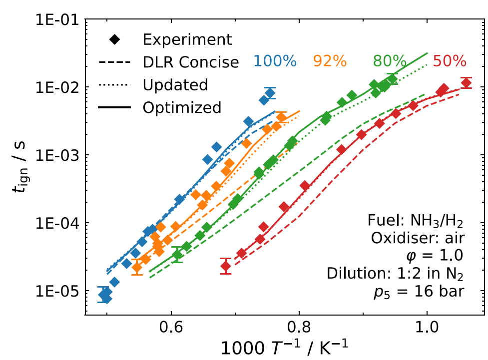

Fig. 5. Ignition delay times from DLR shock tube at 16 bar compared to modeling results with annotations referring to fuel hydrogen content $X_{H2,fuel}$.

models including the elevated collision efficiency of ammonia in R1 are the adapted models and the model Singal2024. Here, the optimized model is in excellent agreement with the experimental data, the model Singal2024 is over-estimating the ignition delay times. All models without the elevated collision efficiency are clearly under-predicting the experimental ignition delay times.

Piston engine modeling results are strongly influenced by the fuel–air mixture ignition delay times at high-pressure in the intermediate temperature regime. With the model adaptations, the simulation results for practical investigated fuel–air mixtures agree with experimental results and significantly shift compared to corresponding modeling results from state-of-the-art reaction mechanisms. Thus, this work's findings on the ignition behavior of ammonia–hydrogen–air mixtures have major implications on applied combustion, especially in numerically aided design of piston engines.

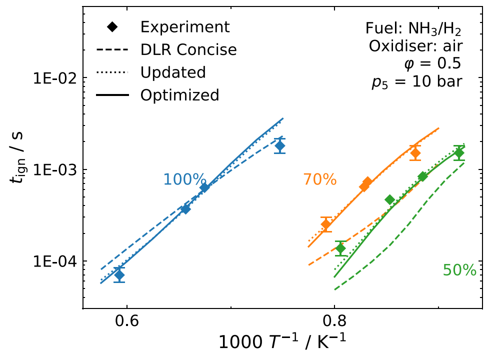

Fig. 6. Ignition delay times from UCF shock tube for lean conditions at 10 bar [6] compared to modeling results with annotations referring to fuel hydrogen content $X_{H2,fuel}$.

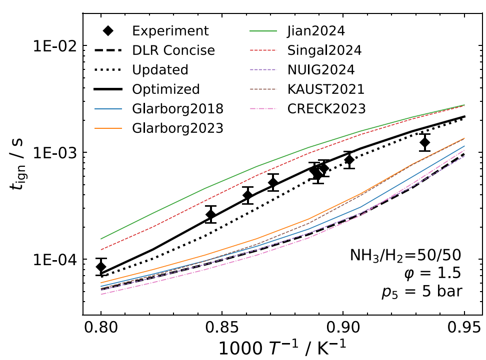

Fig. 7. Ignition delay times from UCF shock tube for rich conditions at 5 bar [6] compared to modeling results.

6. Conclusions

The combined experimental and modeling study on ammonia-hydrogen ignition delay times was able to unravel and solve previous discrepancies between experiments and model predictions for low dilution conditions. The new ignition delay time data confirm the observations of the corresponding UCF data that state-of-the-art reaction models under-predict ammonia–hydrogen ignition delay times for low dilution conditions in the intermediate temperature regime. By adapting the reaction mechanism DLR Concise with well-grounded updates on reaction rates taken from literature, we are able to reproduce the ignition delay times of undiluted fuel–air mixtures from the UCF experiments and the low dilution fuel–air mixtures from the DLR experiments. At the same time, the model agrees well with ignition delay time data available in literature. The model optimization created a new version of the DLR Concise, denoted version *DLRConcise2024v2.F.NH3*. This reaction model was optimized on the comprehensive experimental data set and surpasses the accuracy of literature models on consistently reproducing ignition delay times from shock tubes. Overall, the findings have major implications on the numerical modeling of practical applied combustion applications. This is in particular relevant for the numerically aided design of piston engines, for which engine cycles are highly impacted by ignition delay times in the intermediate temperature regime.

Novelty and significance statement

This research unravels the insufficient modeling performance of state-of-the-art reaction mechanisms for recent experimental data on the ignition behavior for ammonia-hydrogen mixtures under low dilution conditions. With the revision and updating of the model DLR Concise with data from literature, we are able to create a reaction mechanism, consistently modeling low dilution data as well as a broad range of experimental ignition delay times available in literature. The insights are supported and confirmed by new experimental determinations of ammoniahydrogen ignition delay times, measured in shock tubes under intermediate dilutions. The new findings have a significant impact on the modeling of ammonia-hydrogen ignition delay times under real piston engine conditions, leading to strong implications on the future numerical analysis and design of internal combustion engines.

CRediT authorship contribution statement

Torsten Methling: Writing – review & editing, Writing – original draft, Visualization, Validation, Software, Investigation, Formal analysis, Data curation, Conceptualization. **Michael Pierro:** Writing – review & editing, Writing – original draft, Validation, Investigation, Formal analysis. **Nikolas Hulliger:** Writing – review & editing, Writing – original draft, Validation, Investigation, Formal analysis. **Justin J. Urso:** Writing – review & editing, Writing – original draft, Validation, Investigation, Formal analysis. **Jakob Krämer:** Writing – review & editing, Writing – original draft, Visualization, Validation, Data curation. **Clemens Naumann:** Writing – review & editing, Writing – original draft, Validation, Methodology, Investigation, Formal analysis, Data curation, Conceptualization. **Markus Köhler:** Writing – review & editing, Writing – original draft, Funding acquisition. **Subith S. Vasu:** Writing – review & editing, Writing – original draft, Supervision, Funding acquisition, Conceptualization.

Declaration of competing interest

The authors declare that they have no known competing financial interests or personal relationships that could have appeared to influence the work reported in this paper.

Acknowledgments

The University of Central Florida would like to thank the National Science Foundation, United States under Grant NO. OISE1952523 and the U.S. Department of Energy, United States (DE-FE0032172) for supporting this work.

Appendix. Supplementary data

Supplementary material associated with this article can be found in the online version. Attached files include experimental IDTs and non-reactive pressure profiles as tabulated data, the DLR Concise version *DLRConcise2024v2.F.NH3*, the modeling performance on the complete experimental data set (SM1) and sensitivity analyses (SM2).

Supplementary material related to this article can be found online at https://doi.org/10.1016/j.proci.2025.105835.

References

[1] D.F. Davidson, R.K. Hanson, Interpreting shock tube ignition data, Int. J. Chem. Kinet. 36 (9) (2004) 510–523.
[2] D. Nativel, S.P. Cooper, T. Lipkowicz, M. Fikri, E.L. Petersen, C. Schulz, Impact of shock-tube facility-dependent effects on incident- and reflected-shock conditions over a wide range of pressures and Mach numbers, Combust. Flame 217 (2020) 200–211.
[3] O. Mathieu, E.L. Petersen, Experimental and modeling study on the high-temperature oxidation of Ammonia and related NOx chemistry, Combust. Flame 162 (3) (2015) 554–570.
[4] J. Chen, X. Jiang, X. Qin, Z. Huang, Effect of hydrogen blending on the high temperature auto-ignition of ammonia at elevated pressure, Fuel 287 (2021) 119563.
[5] J.B. Baker, R.K. Rahman, M. Pierro, J. Higgs, J. Urso, C. Kinney, S. Vasu, Experimental ignition delay time measurements and chemical kinetics modeling of hydrogen/ammonia/natural gas fuels, J. Eng. Gas Turb. Power 145 (4) (2022).

[6] M. Pierro, C.W. Dennis, A.-A. Pothen, N. Hulliger, T. Kelly, M. Fraze, J.J. Urso, R.K. Rahman, C. Kinney, M. Winquist, J. Vega, G. Subbaraman, R. Steele, S.S. Vasu, Ammonia and ammonia/hydrogen mixtures ignition delay times and chemical kinetic model validation at gas turbine relevant conditions, in: Proc. ASME Turbo Expo, 2024, http://dx.doi.org/10.1115/gt2024-129083, GT2024-129083.

[7] A.G. Szanthoffer, I.G. Zsély, L. Kawka, M. Papp, T. Turányi, Testing of NH_3/H_2 and NH_3/syngas combustion mechanisms using a large amount of experimental data, Appl. Energy Combust. Sci. 14 (2023) 100127.

[8] S. Girhe, A. Snackers, T. Lehmann, R. Langer, F. Loffredo, R. Glaznev, J. Beeckmann, H. Pitsch, Ammonia and ammonia/hydrogen combustion: Comprehensive quantitative assessment of kinetic models and examination of critical parameters, Combust. Flame 267 (2024) 113560.

[9] A. Stagni, S. Arunthanayothin, M. Dehue, O. Herbinet, F. Battin-Leclerc, P. Bréquigny, C. Mounaïm-Rousselle, T. Faravelli, Low- and intermediate-temperature ammonia/hydrogen oxidation in a flow reactor: Experiments and a wide-range kinetic modeling, Chem. Eng. J. 471 (2023) 144577.

[10] X. Zhang, S.P. Moosakutty, R.P. Rajan, M. Younes, S.M. Sarathy, Combustion chemistry of ammonia/hydrogen mixtures: Jet-stirred reactor measurements and comprehensive kinetic modeling, Combust. Flame 234 (2021) 111653.

[11] Y. Zhu, H.J. Curran, S. Girhe, Y. Murakami, H. Pitsch, K. Senecal, L. Yang, C.-W. Zhou, The combustion chemistry of ammonia and ammonia/hydrogen mixtures: A comprehensive chemical kinetic modeling study, Combust. Flame 260 (2024) 113239.

[12] T. Kathrotia, T. Bierkandt, N. Gaiser, S. Richter, F. Lindner, S. Jacobs, C. Naumann, T. Methling, P. Oßwald, M. Köhler, Combustion kinetics of alternative fuels, part-IV: Extending reaction mechanism "DLR concise" to include oxygenates components, Combust. Flame 271 (2025) 113841.

[13] T. Methling, M. Braun-Unkhoff, U. Riedel, A novel linear transformation model for the analysis and optimisation of chemical kinetics, Combust. Theor. Model. 21 (3) (2017) 503–528.

[14] C. Naumann, M. Braun-Unkhoff, P. Frank, A shock tube study on ammonia decomposition and its reaction products, in: 21st International Symposium on Shock Waves, in: Paper 1560, 1997, available at https://elib.dlr.de/3084/, (Accessed 13 March 2025).

[15] J. Herzler, C. Naumann, Shock tube study of the ignition of lean CO/H2Fuel blends at intermediate temperatures and high pressure, Combust. Sci. Technol. 180 (10–11) (2008) 2015–2028.

[16] J.J. Urso, C. Kinney, A.C. Terracciano, S. Barak, A. Laich, M.A. Albright, M. Pierro, J. McGaunn, S.S. Vasu, Characterization of a new ultra-high pressure shock tube facility for combustion and propulsion studies, Rev. Sci. Instrum. 93 (6) (2022) 063905.

[17] T. Kathrotia, P. Oßwald, C. Naumann, S. Richter, M. Köhler, Combustion kinetics of alternative jet fuels, Part-II: Reaction model for fuel surrogate, Fuel 302 (2021) 120736.

[18] P. Glarborg, J.A. Miller, B. Ruscic, S.J. Klippenstein, Modeling nitrogen chemistry in combustion, Prog. Energ. Combust. 67 (2018) 31–68.

[19] A. Kéromnès, W.K. Metcalfe, K.A. Heufer, N. Donohoe, A.K. Das, C.-J. Sung, J. Herzler, C. Naumann, P. Griebel, O. Mathieu, M.C. Krejci, E.L. Petersen, W.J. Pitz, H.J. Curran, An experimental and detailed chemical kinetic modeling study of hydrogen and syngas mixture oxidation at elevated pressures, Combust. Flame 160 (6) (2013) 995–1011.

[20] H. Curran, A comprehensive modeling study of iso-octane oxidation, Combust. Flame 129 (3) (2002) 253–280.

[21] A. Jasper, Predicting third-body collision efficiencies for water and other polyatomic baths, Faraday Discuss. 238 (2022) 68–86.

[22] P.J. Singal, J. Lee, L. Lei, R.L. Speth, M.P. Burke, Implementation of new mixture rules has a substantial impact on combustion predictions for H_2 and NH_3, Proc. Combust. Inst. 40 (1–4) (2024) 105779.

[23] M.U. Alzueta, I. Salas, H. Hashemi, P. Glarborg, CO assisted NH_3 oxidation, Combust. Flame 257 (2023) 112438.

[24] J. Jian, H. Hashemi, H. Wu, P. Glarborg, A.W. Jasper, S.J. Klippenstein, An experimental, theoretical, and kinetic modeling study of post-flame oxidation of ammonia, Combust. Flame 261 (2024) 113325.

[25] S.J. Klippenstein, P. Glarborg, Theoretical kinetics predictions for NH_2 + HO_2, Combust. Flame 236 (2022) 111787.

[26] A. Stagni, C. Cavallotti, S. Arunthanayothin, Y. Song, O. Herbinet, F. Battin-Leclerc, T. Faravelli, An experimental, theoretical and kinetic-modeling study of the gas-phase oxidation of ammonia, Reac. Chem. Eng. 5 (4) (2020) 696–711.

[27] P. Marshall, G. Rawling, P. Glarborg, New reactions of diazene and related species for modelling combustion of amine fuels, Mol. Phys. 119 (17–18) (2021) e1979674.

[28] S.J. Klippenstein, L.B. Harding, B. Ruscic, R. Sivaramakrishnan, N.K. Srinivasan, M.-C. Su, J.V. Michael, Thermal decomposition of NH2OH and subsequent reactions: Ab initio transition state theory and reflected shock tube experiments, J. Phys. Chem. 113 (38) (2009) 10241–10259.

[29] P. Glarborg, The $NH_3/NO_2/O_2$ system: Constraining key steps in ammonia ignition and N_2O formation, Combust. Flame 257 (2023) 112311.

[30] T. Methling, M. Braun-Unkhoff, U. Riedel, An optimised chemical kinetic model for the combustion of fuel mixtures of syngas and natural gas, Fuel 262 (2020) 116611.

[31] D.L. Baulch, C.T. Bowman, C.J. Cobos, R. Cox, T. Just, J.A. Kerr, M.J. Pilling, D. Stocker, J. Troe, W. Tsang, R.W. Walker, J. Warnatz, Evaluated kinetic data for combustion modeling: Supplement II, J. Phys. Chem. Ref. Data 34 (3) (2005) 757–1397.

[32] D.G. Goodwin, H.K. Moffat, I. Schoegl, R.L. Speth, B.W. Weber, Cantera: An object-oriented software toolkit for chemical kinetics, thermodynamics, and transport processes, 2023, https://www.cantera.org. Version 3.0.0, (Accessed 12 March 2025).

[33] T.L. Nguyen, J.F. Stanton, Ab initio thermal rate coefficients for $H + NH_3 \rightleftharpoons H_2 + NH_2$, Int. J. Chem. Kinet. 51 (5) (2019) 321–328.

[34] S. Salimian, R.K. Hanson, C.H. Kruger, High temperature study of the reactions of O and OH with NH3, Int. J. Chem. Kinet. 16 (6) (1984) 725–739.

[35] G. Altinay, R.G. Macdonald, Determination of the rate constants for the $NH_2(X^2B_1)$ + $NH_2(X^2B_1)$ and $NH_2(X^2B_1)$ + H recombination reactions in N_2 as a function of temperature and pressure, J. Phys. Chem. 119 (28) (2015) 7593–7610.

[36] S.J. Klippenstein, L.B. Harding, P. Glarborg, J.A. Miller, The role of NNH in NO formation and control, Combust. Flame 158 (4) (2011) 774–789.

[37] S. Song, R.K. Hanson, C.T. Bowman, D.M. Golden, Shock tube determination of the overall rate of $NH_2 + NO \rightarrow$ products in the thermal De-NOx temperature window, Int. J. Chem. Kinet. 33 (11) (2001) 715–721.